This article has been accepted for publication in a future issue of this journal, but has not been fully edited. Content may change prior to final publication. Citation information: DOI 10.1109/TAP.2015.2435037, IEEE Transactions on Antennas and Propagation

A High Power Microwave Zoom Antenna with Metal Plate Lenses

J. Lawrance, C. Christodoulou, M. R. Taha

***Abstract*—Metal plate lens antennas were designed and constructed for a high power microwave zoom antenna concept comprising a pyramidal horn feed antenna and two metal plate lenses. Good agreement was found between experiment and simulation. This antenna provides true zoom capability with continuously variable collimated beam output, approximately 10% bandwidth, and very high power handling capability. It can be designed to operate at any frequency in the range of about 100MHz to 10GHz. It was found that nano-modified carbon fiber composites could be used instead of metal plates in these lenses; these composites would reduce the weight of the lens significantly and would help to mitigate possible spurious TM modes induced in the lens when it is in the near field of the feed horn antenna.**

***Index Terms*—Zoom antennas, metal plate lenses, parallel plate waveguide lenses, high power microwave zoom antenna**

I. INTRODUCTION

A true zoom antenna produces a collimated beam of electromagnetic (EM) energy with a planar wavefront and with continuously variable diameter. This type of antenna provides beam control in terms of spot size and power density on target. A true high power microwave (HPM) zoom antenna greatly extends the range of an HPM source and is useful for such applications as target acquisition and tracking, and communications. Until now, true zoom antenna capability for high power microwave applications did not exist.

The zoom antenna concept presented herein and in [1] consists of a horn feed antenna and two metal plate lenses. These lenses are particularly well suited to this application. While aluminum was originally the metal of choice for these lenses, newly emerging carbon fiber reinforced polymer (CFRP) composites were demonstrated in simulation to have sufficient conductivity for this application and bear further study. These compounds have lower density than aluminum; they provide a lightweight alternative to metal for lens construction, which becomes important for applications at lower frequencies

This effort comprised design and demonstration – through experiment and simulation - of a true zoom antenna concept for HPM applications. This is a narrowband antenna with approximately 10% bandwidth which produces a linearly polarized collimated beam with continuously variable diameter (achieved by axial translation of the lenses relative to each other and relative to the feed horn). The zoom antenna can be designed for a wide range of frequencies from hundreds of megahertz (MHz) to tens of gigahertz (GHz). It has excellent power handling capability: ranging from tens of megawatts (MW) at 10GHz to several gigawatts (GW) at 1GHz.

This is a practical system that could be implemented in the field near-term. Design considerations and analysis are focused on minimizing complexity and cost of fabrication. However, if minimizing weight is an issue, carbon fiber compounds should be considered for lens construction.

II. BACKGROUND

Historically, the term "zoom antenna" has been erroneously applied to reflector antennas that are used to broaden the beam through a defocusing effect; there are a number of these types of antennas described in available literature and existing patents; some examples are given in [2-4]. These are not technically zoom antennas. While Cassegrain and Gregorian (reflector) antennas can produce a collimated beam of electromagnetic energy; they cannot provide continuously variable diameter of this collimated beam. True zoom capability cannot be achieved with any of these reflector type antennas.

A true high power microwave (HPM) zoom antenna therefore requires the use of lenses. Dielectric lenses are not a good option for HPM applications because they are lossy at high frequencies and because they become prohibitively heavy at lower frequencies on the order of a few gigaherz. Metal plate lenses are particularly well-suited to the HPM zoom antenna application.

The concept of the metal plate lens was proposed by W.E. Kock [5] in the 1940's; however, it has found limited application since. More detailed discussion of these lenses is found in [6-9]. According to Kraus, [10], one of the major benefits of parallel plate waveguide lenses (or what he refers to as "E-plane metal plate lens antennas") over parabolic reflectors is that the tolerance of this type of lens is much higher than the surface contour requirements of a parabolic reflector such that, "a relatively large amount of warping and twisting can be tolerated". This is a major benefit for a practical system that can be implemented in the field, and, in fact, this was demonstrated to be true in experiments presented herein.

A drawback of these lenses, according to Kraus, is their small bandwidth. He derives in [6] a bandwidth on the order of 5% [10]; however, this is based on an arbitrarily chosen value

This article has been accepted for publication in a future issue of this journal, but has not been fully edited. Content may change prior to final publication. Citation information: DOI 10.1109/TAP.2015.2435037, IEEE Transactions on Antennas and Propagation

for path length error tolerance and the useable bandwidth may be closer to 10%. This is discussed further in Section IV of this paper.

Single metal plate lenses have been designed and implemented by HAM radio operators to extend the range of radar guns [11]. They have also been implemented in experiments designed to explore interaction of HPM energy with plasmas. It is thought that they were once used as boosters in telecommunications systems; however documented evidence of this is not readily available.

Implementing these lenses in a high power microwave zoom antenna has not been proposed or demonstrated prior to this work.

III. THEORY – ZOOM ANTENNA CONCEPT

This paper presents results of experiment and simulation exploring application of metal plate lenses to a high power microwave zoom antenna concept. This antenna consists of three elements: a pyramidal horn feed antenna and two appropriately designed parallel plate waveguide spherical lenses that can be translated along the boresight axis relative to each other and relative to the phase center of the feed horn. The output of this antenna system is a variable diameter (TEM) collimated beam output. The antenna works for linear polarization and the bandwidth is on the order of 10%. While it is a narrowband antenna; it can be designed to operate at any frequency in the range of about 100 MHz to 10GHz.The metal plate lens antenna, shown conceptually in Fig. 1, is essentially a parallel plate waveguide array antenna through which electromagnetic energy propagates in the TE1 mode when the incident electric field vector is parallel to the plates.

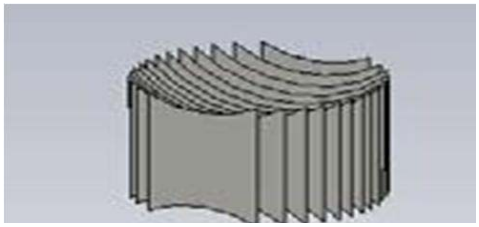

Fig. 1 Conceptual illlustration of metal plate lens.

It consists of an array of parallel metal plates with constant spacing "a". When "a" is slightly greater than half a wavelength, the index of refraction of the structure, *n*, is less than 1. The index of refraction [5] is determined by

$$n = \sqrt{1 - \left(\frac{\lambda}{2a}\right)^2} \tag{1}$$

where λ is the wavelength. The front and back faces of the metal plate array can then be shaped to provide the desired focal length, *f*, according to the thin lens approximation to the lensmaker's equation:

$$\frac{1}{f} = (n-1)\left(\frac{1}{R1} - \frac{1}{R2}\right) \tag{2}$$

where R1 and R2 are the radii of curvature of the front and back faces of the lens.

Positioning of the lenses to achieve a collimated (pencil beam) output is governed by

$$\frac{1}{f} = \frac{1}{S1} + \frac{1}{S2} \tag{3}$$

where S1 is the distance from the phase center of the pyramidal feed horn antenna and S2 is the distance from the center of lens 1 to the center of lens 2, as shown in Fig. 2.

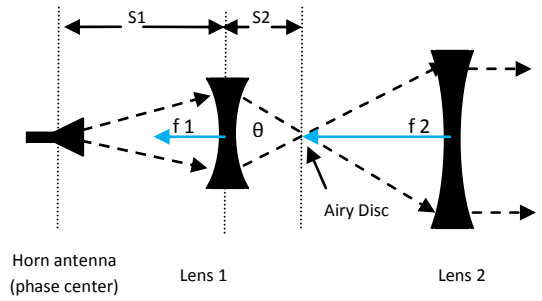

Fig. 2 Zoom antenna concept – broad collimated beam output.

Reducing the diameter of the collimated beam output of the zoom antenna is achieved by repositioning the lenses such that lens one is closer to the phase center of the horn antenna (while still being greater than a focal length, f1, away) and such that lens 2 is again one focal length, f2, from the new location of the focal plane of lens 1. This is illustrated graphically in Fig 3.

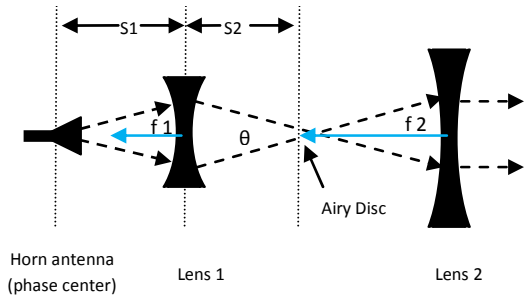

Fig. 3 Zoom antenna concept – narrow collimated beam output.

In the focal plane of lens 1, the beam is not focused to a point, but is diffraction limited to an Airy disc, with a diameter, x, [12] is determined by

$$x = \lambda \frac{f}{d} \tag{4}$$

where f is the focal length and d is the diameter of the lens.

This article has been accepted for publication in a future issue of this journal, but has not been fully edited. Content may change prior to final publication. Citation information: DOI 10.1109/TAP.2015.2435037, IEEE Transactions on Antennas and Propagation

IV. Experimental and Simulated Results

To demonstrate the zoom concept, a pair of 10-GHz metal plate spherical lenses were designed and built: a biconcave lens with a diameter of 40.6 cm and a focal length of 25.4 cm and a larger plano concave lens with a diameter of 81.3 cm and a focal length of 139.7 cm. The plate spacing of the lenses was 1.9 cm, resulting in an index of refraction of 0.6. A 15dBi horn antenna was appropriately placed and driven by port 1 of a network analyzer. The lenses thus built were low power lenses; constructed with insulated foam sheathing providing the spacing between the lens elements and aluminum foil for the lens plates. The lenses were positioned to achieve a collimated beam output. Low power S21 measurements were made with a small receive horn antenna connected to port 2 of the network analyzer across the focal plane of the first lens in the E- and H-planes as well as at the output of the antenna along boresight. The entire system (including the horn antenna and both lenses) was simulated and the results showed good agreement.

To measure beam collimation, the lenses were appropriately positioned relative to the feed horn antenna and S21 measurements were made along boresight in the near field at the output of the zoom antenna system. These measurements were then repeated with the lenses removed. The results were compared and are shown in Fig 4. Without the lenses, $1/r^2$ loss was observed. With the lenses in place, the power remains relatively constant with distance moving away from the antenna, indicating beam collimation. There is some drop in power seen in the upper curve of Fig. 4; however this approximately 2-3dB decrease across the measurement range out to 5500mm is believed to be caused by imperfect placement and alignment of the lenses which was accomplished to the best of the author's ability using a plumb bob, tape measure and line of sight. It is expected that beam collimation will sustain over the near field which, for this 10GHz zoom antenna system (whose largest dimension is on the order of 1200 mm from feed horn to lens 2) greatly exceeds the distance over which these measurements were made. Sustainment of beam collimation at the output of the zoom antenna in the near field is supported by the results of simulation presented in the next section. Of course, in the far field, power along boresight is expected to fall as $1/r^2$.

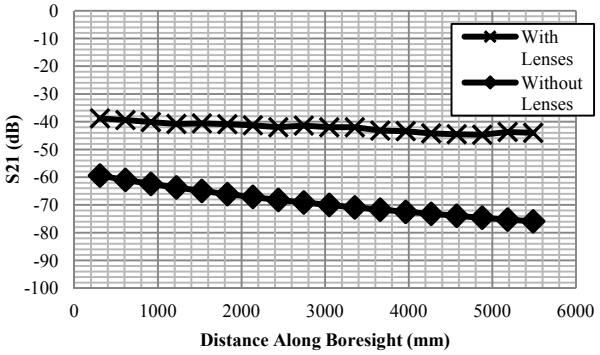

Fig. 4 Boresight measurements with and without lenses

More experimentally measured results for the zoom antenna are shown in Fig. 5 and Fig. 6, which present normalized S21 measurements across the E- and H- planes, respectively, across a plane orthogonal to boresight at a distance of 3 meters from the second lens ; with the lenses positioned for a relatively narrow collimated beam. The solid lines in these figures correspond to a second order polynomial best fit curve to the data, shown by the "x's".

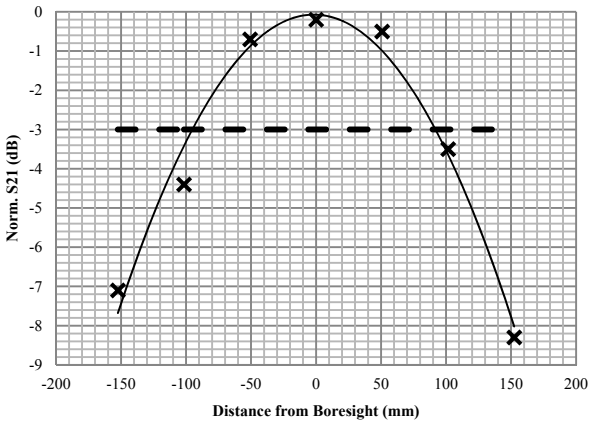

Fig. 5 Normalized S21 measurements across E-plane (narrow collimated beam)

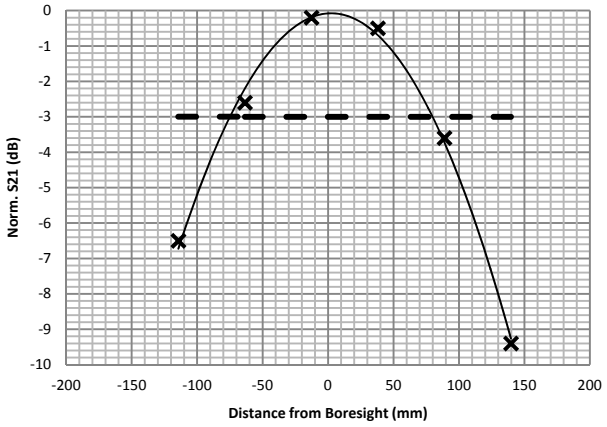

Fig. 6 Normalized S21 measurements across H-plane: narrow collimated beam

As can be seen in Fig. 5 and Fig. 6, the half power beam width for the narrow collimated beam in these experiments was on the order of 190 mm.

These same measurements were made at a distance of 3 meters from the second lens with the lenses re-positioned to achieve a relatively broad collimated beam; the results are shown in Fig. 7 and Fig. 8, for the E- and H- planes, respectively. Again, the solid lines in these figures correspond to a second order polynomial best fit curve to the data, shown by the "x's".

The measurements indicate a half power beamwidth in this case of close to 500mm. The wavefront is not as well behaved

This article has been accepted for publication in a future issue of this journal, but has not been fully edited. Content may change prior to final publication. Citation information: DOI 10.1109/TAP.2015.2435037, IEEE Transactions on Antennas and Propagation

for the broad collimated beam, as can be seen in these figures. To achieve this broadest collimated beam, lens 1 is at its furthest point from the feed horn. At this distance, phase difference between the central and outer rays of the beam from the feed horn antenna starts to become significant; however, because this is a dynamic system, reshaping the lenses to achieve phase compensation at the farthest lens 1 position affects the phase front of the wave when lens 1 is nearest to the aperture of the horn antenna.

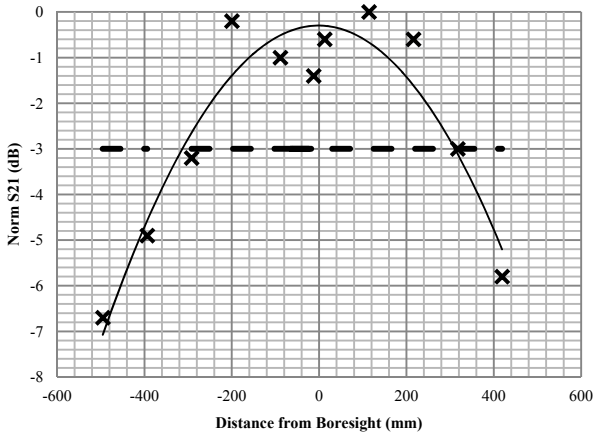

Fig. 7 Normalized S21 measurements across E-Plane (broad collimated beam)

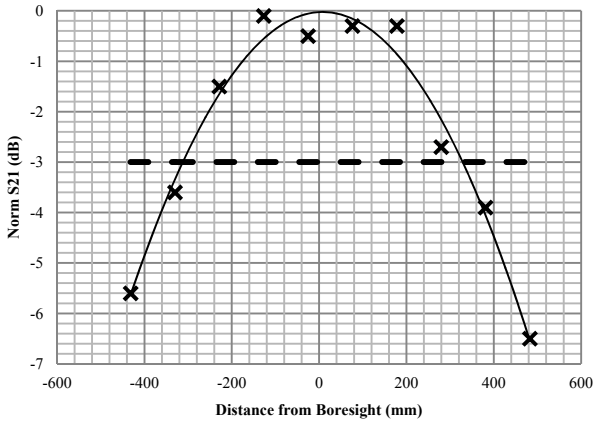

Fig. 8 Normalized S21 measurements across H-Plane (broad collimated beam)

Simulated measurements of the zoom antenna are shown in Fig. 9 through Fig. 11. In these simulations, propagation is in the y-direction and the electric field is in the x direction. The feed horn is located at the bottom of the picture, pointing upward. The feed horn and lenses were constructed for these simulations using the same design parameters as the horn and lenses constructed for the experimental measurements. The lenses were modeled in detail using the same dimensions as the actual lenses constructed for testing, with the plate material simulated as perfect electric conductor (PEC).

In Fig. 9, the x-directed electric fields in the x-y plane (E-plane) reveal high fields (in red) in and near the feed horn. The lens (in white) is greater than a focal length away from the phase center of the horn antenna. Focusing of the fields can be seen in the elongated red strip above the lens in this figure. In the realm of optics, this is referred to as the "confocal region", or "depth of field". The Airy disk in the focal plane is located in this strip in a plane orthogonal to the direction of propagation.

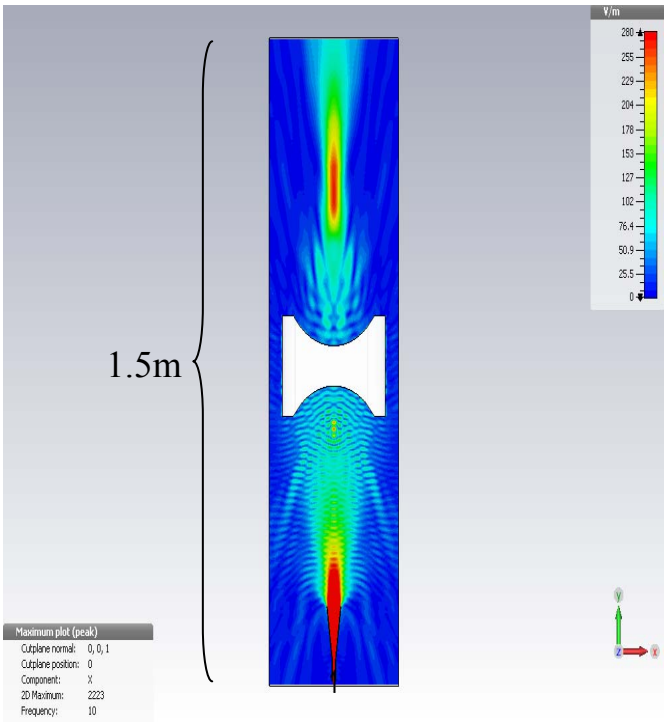

Fig. 9 Focusing of beam beyond lens 1

In Fig. 10 and Fig.11, the electric fields in the x-y plane (E-plane) for the full zoom antenna including two lenses are presented. In Fig. 10, the lenses are positioned to achieve a narrow collimated beam. The same confocal region is observed beyond lens 1. Beyond lens 2, the beam settles down to a collimated beam at the output, near the top of the picture. In Fig. 10, the width of the collimated beam of lens 2 is relatively narrow. In Fig. 11, with lens 1 positioned farther from the phase center of the feed horn (and lens 2 re-positioned to be a focal length, f2, from the focal plane of lens 1), the width of the collimated beam beyond lens 2 is larger. These simulations cover a boresight distance out to 5000 mm. The nicely collimated beam evident in the simulations at y = 5000 mm supports the observation in Section IV of this paper that beam collimation over the near field is achieved with this zoom antenna. It should be noted here that the largest dimension of this zoom antenna is the distance from the feed horn antenna to the second lens; approximately 2.45-3.0 m for this 10GHz zoom antenna, while the wavelength is only 0.03 m. This results in a large Fraunhofer distance.

This article has been accepted for publication in a future issue of this journal, but has not been fully edited. Content may change prior to final publication. Citation information: DOI 10.1109/TAP.2015.2435037, IEEE Transactions on Antennas and Propagation

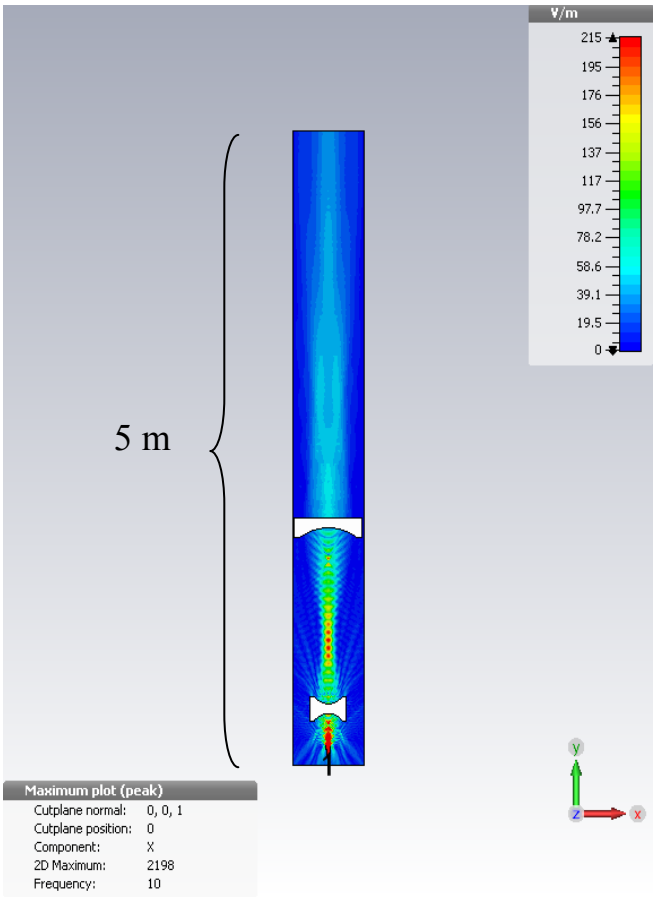

Fig. 10 Zoom antenna – narrow collimated beam

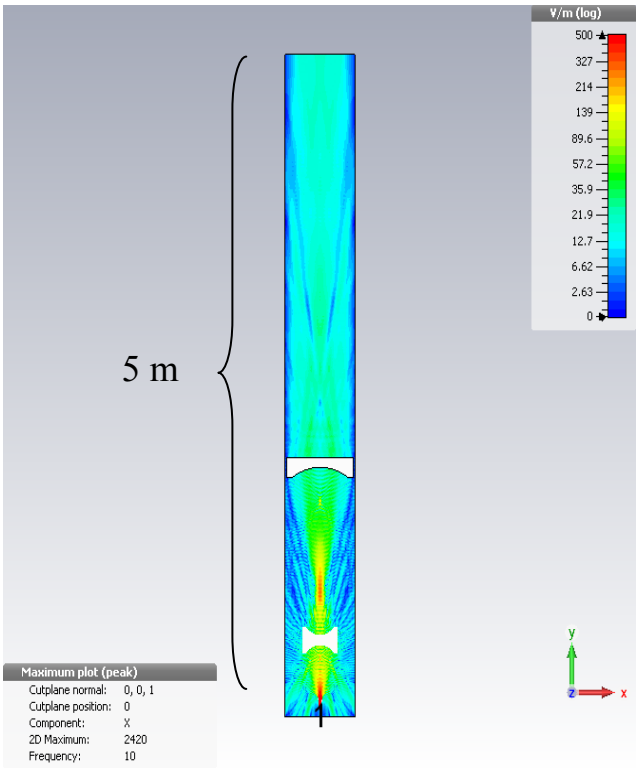

Fig. 11 Zoom antenna – broad collimated beam

Backscatter occurs off the plates and there is also a reflection due to mode mismatch at the air-lens interface; however there is not much that can be done to mitigate this.

The bandwidth of this system is determined primarily by the fact that the index of refraction of the lens is dependent on wavelength and the focal length therefore changes with frequency. Too large of a variation will affect the overall operational characteristics of the zoom antenna.

To illustrate, the variation in index of refraction for a lens designed to operate at 10 GHz with an index of refraction close to 0.65 is shown in Fig. 12. A ±5% variation in frequency (for an overall bandwidth of 10%) will result in a ±5% variation in index of refraction and a ±5% variation in focal length of the lens. For a practical zoom antenna, the focal length of lens 1 will be on the order of 10 wavelengths. A ±5% variation in focal length would result in at most a half wavelength of variation in the focal length of lens 1. The focal length of lens 2 for a practical system is on the order of 50 wavelengths. A five percent difference in the focal length of lens 2 would therefore correspond to 2.5 wavelengths; however, it is important to note here that the depth of the confocal region between lens 1 and lens 2 is on the order of 10 wavelengths in Fig. 10, and this is tolerated by the zoom antenna system as evidenced by its ability to achieve collimation as seen in Figs. 10 and 11. It is therefore expected that a practical zoom antenna would operate well with a high power microwave source with up to a 10% bandwidth. This is supported by [8] in which a bandwidth of > 10% is derived for a metal plate lens with index of refraction n > 0.5.

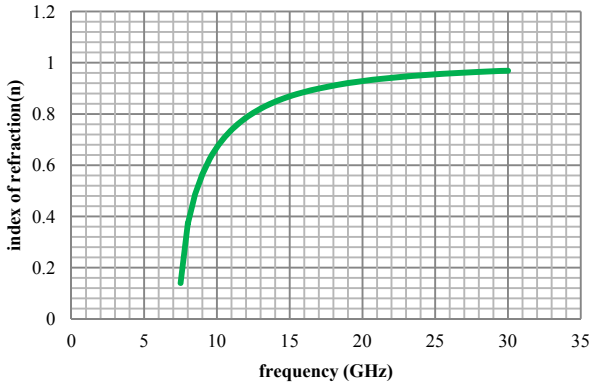

Fig. 12 Dependence of index of refraction on frequency

A high power lens was constructed as shown in Fig. 13 to demonstrate power handling capability. The plates were 1/16" (1.6 mm) aluminum; dielectric rods and spacers were included for structural support. This was an L-Band lens with a diameter of 1.8 meters and a width of 1.2 meters. The feed horn used was a high power horn antenna. An s-band open waveguide was used as the sensor, shown mounted on a tripod in Fig. 13 to attenuate the receive signal. The source power was 200 MW; it delivered a 1μs pulse to the antenna.

This article has been accepted for publication in a future issue of this journal, but has not been fully edited. Content may change prior to final publication. Citation information: DOI 10.1109/TAP.2015.2435037, IEEE Transactions on Antennas and Propagation

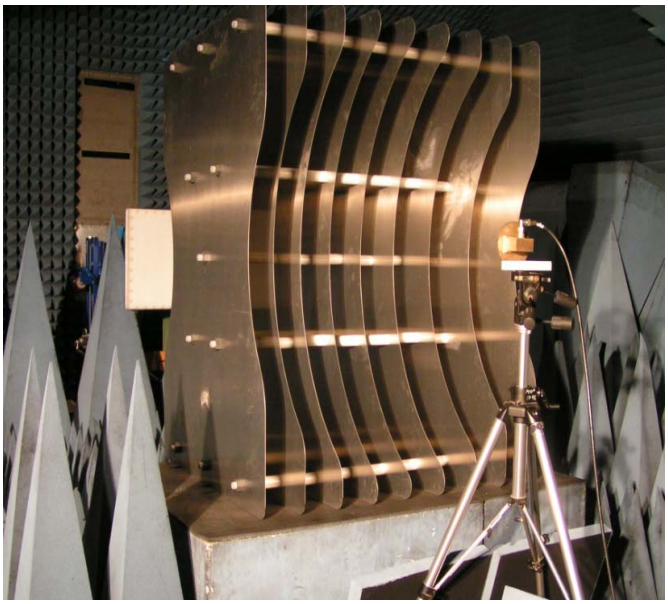

Fig. 13 High power L-Band metal plate lens

Boresight measurements were made by moving the S-band receive sensor along boresight in increments away from the lens, through the confocal region produced by the lens. They were then repeated with the lens removed, for comparison. The results are shown in Fig. 14. With the lens in place, denoted by x's in Fig. 14, the S21 measurement peaks at a distance of about 2m from the lens. Note also the length of the confocal region for this lens in Fig. 14 of approximately 300mm or about 10 wavelengths. With the lens removed, the S21 measurement falls steadily, corresponding to 1/r2 loss in power with increasing distance from the horn antenna.

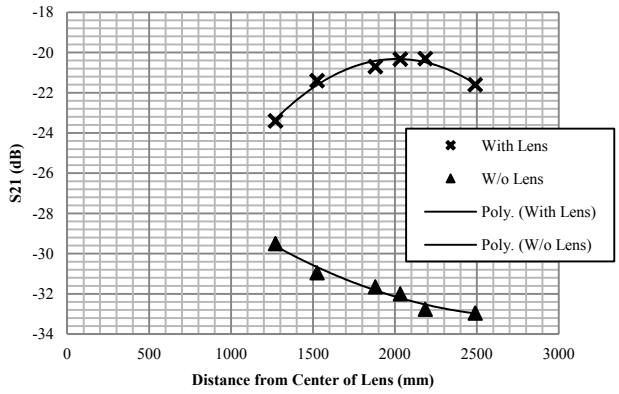

Fig. 14 Boresight measurements, L-band high power lens

Measurements were then made across the focal plane in the E- and H-planes. The results are shown in Fig. 15 and Fig. 16. These measurements indicate a half power beamwidth of close to 330 mm in both planes. The free space wavelength at the center frequency of the source was 230mm; the half power beamwidth across the Airy disc was therefore close to 1.5 λ.

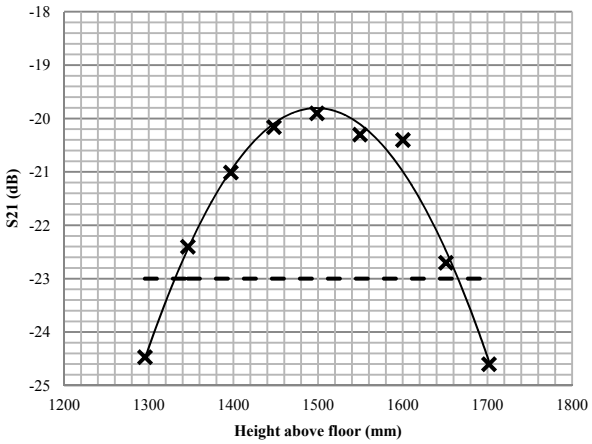

Fig. 15 Electric Field across focal plane (E-plane) w/lens at 2.56m from horn aperture

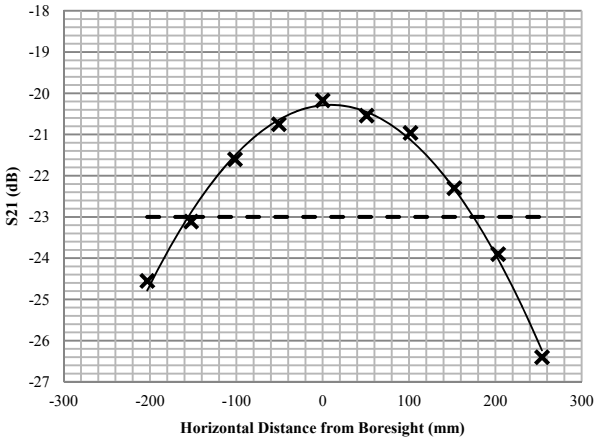

Fig. 16 Electric field across focal plane (H-plane) with lens at 2.56m from horn aperture

The power handling capability of the system is limited, for pulsed operation, by the dielectric strength of air, or 3 x 10^3 kV/m. High electric fields exist within the focal region created by lens 1 and are a maximum at the center of the this focal plane.

If all of the source power (P_s) were to be concentrated over the area of the Airy disc created by lens 1, the average power density in this disc, $S_{ave,}$ assuming 70% efficiency of the lens, would be:

$$S_{ave} = \frac{0.7P_s}{A} \quad (5)$$

where A is the area of the Airy disk. The diameter of this disc was demonstrated through experiment and simulation spanning 1-10GHz to have a diameter of close to 1.5λ, so that the area of this disc is.

$$A = 4\pi(.75\lambda)^2 \quad (6)$$

This article has been accepted for publication in a future issue of this journal, but has not been fully edited. Content may change prior to final publication. Citation information: DOI 10.1109/TAP.2015.2435037, IEEE Transactions on Antennas and Propagation

Since the diameter of this disc is defined as the half power beamwidth, the peak power density in the center of the disc, S_p would be twice the average power density, or $S_p = 2S$.
The peak electric field in air (having an impedance of 377 Ω), is then determined from

$$E = \sqrt{377 S_p} \tag{7}$$

Or

$$E = \sqrt{377(2S)} \tag{8}$$

So that the peak electric field in the center of the disc is

$$E = \sqrt{377 \frac{0.7 * 2 * P_s}{4\pi(.75\lambda)^2}} \tag{9}$$

where the factor of 0.7 is included to account for the efficiency of the lens. Therefore, the source power required to cause air breakdown in the center of the disc is determined from

$$P_s = \frac{E^2(4\pi(.75\lambda)^2)}{(377)(1.4)} \tag{10}$$

This curve is shown in Fig. 17.

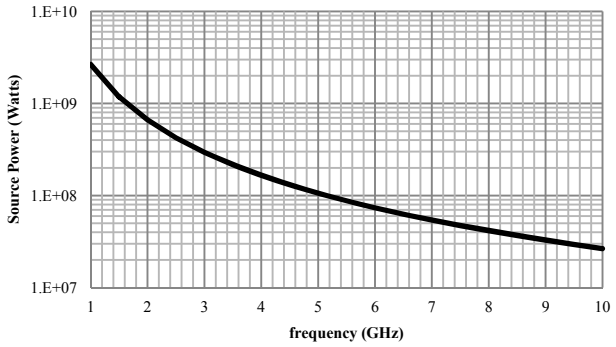

Fig. 17 Source power required to induce air breakdown

For the lens plates, it is desirable to have high conductivity, low density to minimize weight, low reactivity with air/water for outdoor applications, and sufficient rigidity and strength to maintain their shape with the type of construction shown in Fig. 13; i.e., built for very high power applications, with air spacing and dielectric rod support structures.

Aluminum has long been the material of choice for many antenna components due to its high conductivity, relatively low reactance with air and water, light weight, and low cost.

However, newly emerging carbon fiber reinforced polymer (CFRP) composites may provide a better alternative to aluminum in terms of strength and weight, especially for lower frequency applications where the dimensions of the antenna become relatively large. These composites have been explored for applications that include slotted waveguide arrays and microstrip antennas [13,14] and their conductivity/resistivity has been evaluated analytically [15-17] and measured experimentally [18, 19]. These have sufficient rigidity and tensile strength to serve as lens plates, and could significantly reduce the weight of the lenses, provided they have sufficient conductivity.

To investigate, simulations were run to explore the minimum conductivity required for the lens plates. The setup for the simulation is shown in Fig. 18. The feed horn was designed to have a gain of 16dBi and had a waveguide feed sufficiently long to support the TE10 mode of propagation. A waveguide port was applied to the input at y = 0. The direction of propagation is in the y-direction and the electric field is in the x-direction in these simulations.

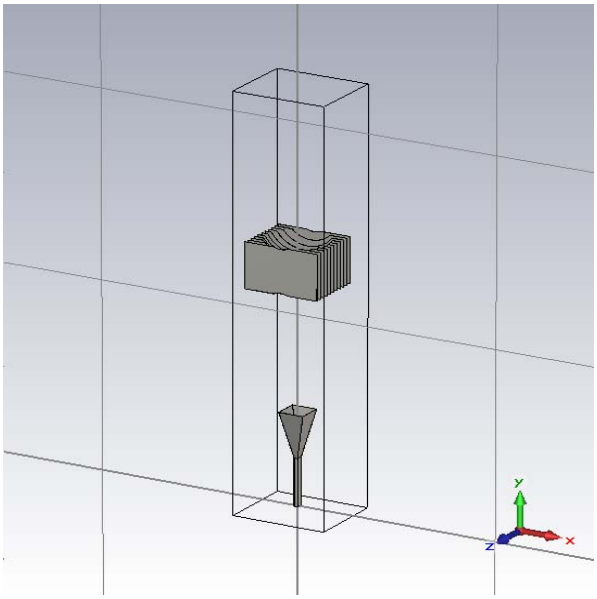

Fig. 18 Simulation setup with feed horn and single parallel plate waveguide array lens

The waveguide port was then excited with a Gaussian excitation of 1-2 GHz. This frequency range was selected because weight reduction becomes more important at lower frequencies as lens size increases and because the conductivity of a material increases with frequency (as skin depth increases). Therefore, showing sufficient conductivity at the lower end of the frequency range is sufficient to establish that this conductivity would suffice at higher frequencies.

The DC conductivity of the Carbon Fiber Reinforced Polymer Composite material was provided by the manufacturer and is shown in Fig. 19, relative to aluminum plate, foil, and bulk aluminum. The DC conductivity was measured at 726 S/m.

This article has been accepted for publication in a future issue of this journal, but has not been fully edited. Content may change prior to final publication. Citation information: DOI 10.1109/TAP.2015.2435037, IEEE Transactions on Antennas and Propagation

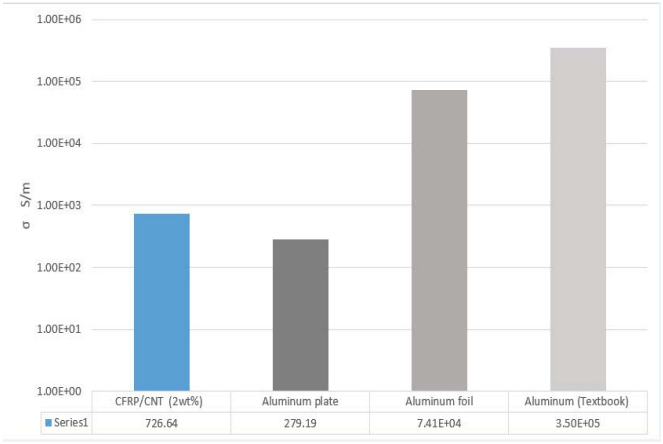

Fig. 19 Conductivity of CFRP/CNT compared to aluminum

The thickness of the plates was arbitrarily chosen to be 3 mm (1/8th inch) for these simulations, although thinner plates would work just as well, limited only by the skin depth of the material at the lowest operational frequency.

Several simulations were run, each time changing the material properties to vary the conductivity of the material. Wave propagation from the horn antenna and through the lens to beyond the focal plane was simulated for infinite conductivity (corresponding to that of a PEC), with a conductivity of 726 S/m (corresponding to that of the UNM CFRP composite), and with arbitrary materials having conductivities of 10 and 100 S/m. The results are shown in Figs. 20 and 21 which show the electric field across the E and H planes for each of these materials. Because the material having a conductivity equal to that of the UNM CFRP material does not significantly affect the peak electric field nor the width of this field in the focal region of the lens, this material is not too lossy for this application.

In addition, this material would reduce the weight of the lens by 25% or more and would have sufficient tensile strength and rigidity to replace aluminum for lens design.

While inclusion of CFRP composites in the design of the parallel plate waveguide lenses may add to the cost, the reduction in weight may be desirable. The density of the CFRP/CNT composite was approximately 25% less than the density of aluminum . Therefore the reduction in weight would be about 25%. However, since it was demonstrated herein that even lower conductivity would work well as lens plates, this weight could be reduced even further.

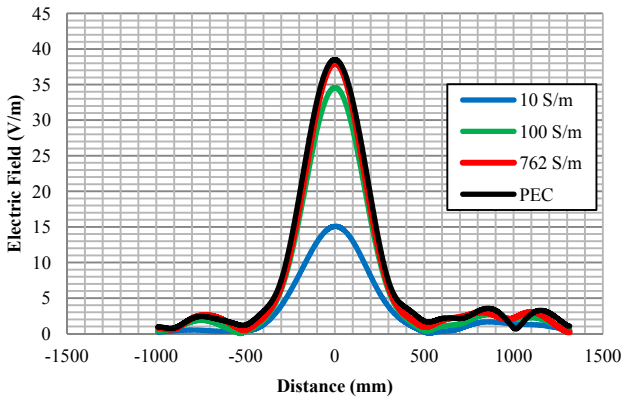

Fig. 20 E-plane measurements in the focal plane

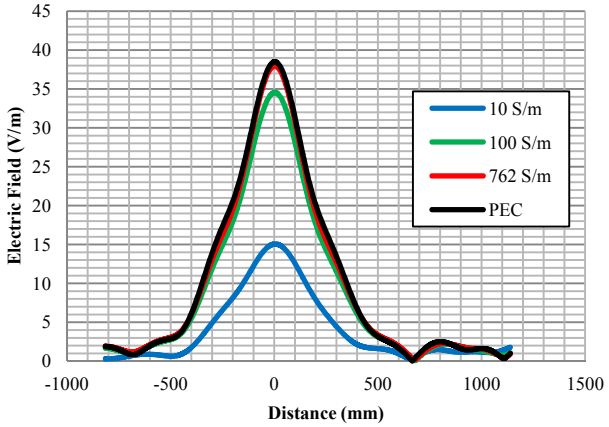

Fig. 21 H-Plane Measurements Across Focal Plane

The use of such a carbon fiber composite in the construction of the lenses may have an additional important benefit. Spurious modes could be induced in the parallel plate waveguide lens by the presence of longitudinal or cross polarized fields which might exist in the near-field of the pyramidal feed horn antenna. These could adversely affect the focusing capability of the lens.

As mentioned previously, the plate spacing for the lens was chosen to be slightly larger than ½ λ at the center frequency, and such that the index of refraction is very close to n = 0.6. This ensures propagation in the TE1 mode, for which the cutoff frequency is

$$f_c(\mathrm{TE1}) = \frac{c}{2a} \qquad (11)$$

It is important to note that this is also the cutoff frequency for the TM1 mode.

In the near field of the horn, undesirable longitudinal and transverse electric fields (in the y- and z- directions in the simulations) could exist; exciting unwanted TM or TEM modes in the parallel plate waveguide structure of the lens.

This article has been accepted for publication in a future issue of this journal, but has not been fully edited. Content may change prior to final publication. Citation information: DOI 10.1109/TAP.2015.2435037, IEEE Transactions on Antennas and Propagation

The X-band horn used in the simulations is shown in Fig. 22, along with an electric field monitor placed in the near field of the horn about a wavelength away from the aperture.

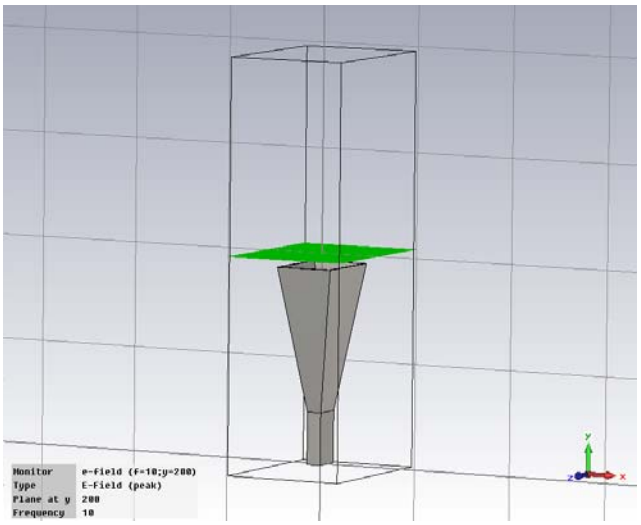

Fig. 22 X-Band Horn with Field Monitor in the Near Field (y = 200mm)

Electric fields in the x-, and z-directions were evaluated in the plane of this field monitor as well as in the E-plane (z = 0).

The magnitude of the x-directed E-field in the plane of the field monitor at y = 200mm is shown in Fig. 23. It is relatively constant over a rectangular area in the x-z plane and has a magnitude of 457 V/m. This is the desirable component of the electric field and appears well behaved across the aperture of the horn.

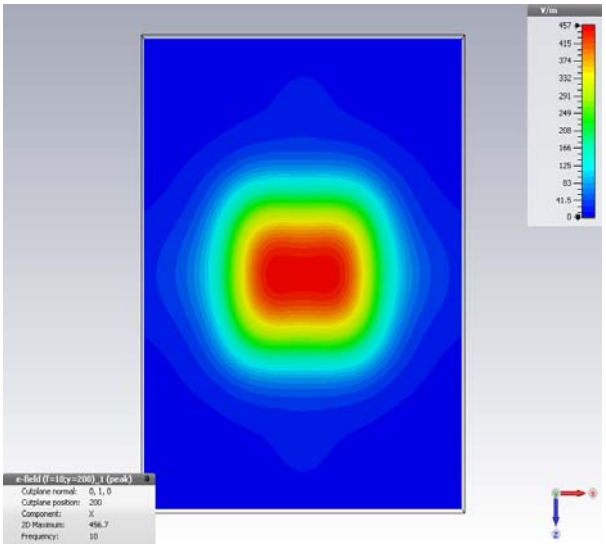

Fig. 23 Near Field Electric Field (E_x)

The z-component of the electric field, which would tend to propagate through the lens in the TEM mode, was found to be on the order of a factor of 10 down from the peak x-directed E-fields and is not significant.

The y-component of the electric field (longitudinal component), however, was found to be significant and is shown in the E-plane in Fig. 24. The peak field is split into two regions and has a peak magnitude of 155 V/m.

This longitudinal component is only a factor of three down from the peak x-directed electric field at a distance of about a wavelength from the aperture of the horn. This has the potential to excite TM modes in the waveguide when the lens is very close to the horn aperture; the fundamental TM1 mode has the same cutoff frequency as the TE1 mode for parallel plate waveguide and hence the same propagation velocity.

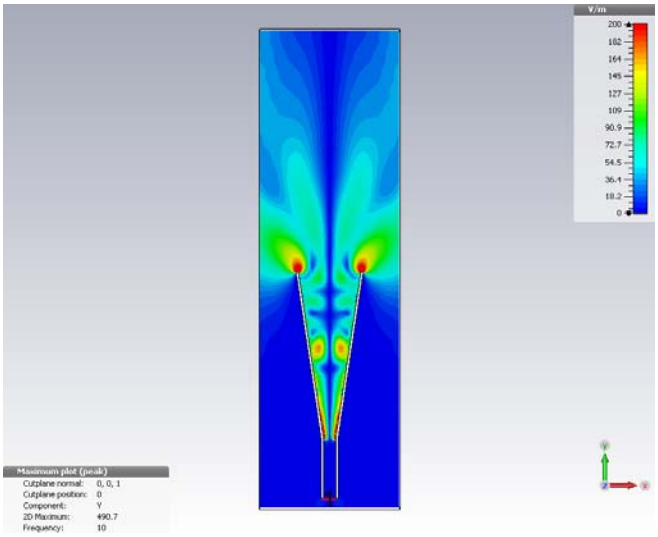

Fig. 24 Longitudinal Fields Ey in the X-Y Plane

Note the high intensity electric fields observed at the edges of the horn antenna along the aperture in Fig. 24. These are easily mitigated by attaching a rolled surface section to the outside of the horn and will therefore not be discussed further here; except to say that the shape is not critical but that its radius of curvature should be larger than λ/4 [20].

The y-directed electric fields would propagate on the outer portion of the lens and could affect the beam pattern in the focal plane of the lens.

Interestingly, some finite resistivity to the plates may help to mitigate spurious modes induced by longitudinal fields in the near field of the horn antenna. The attenuation due to conductor loss for the TEM, TE1 and TM1 modes is presented in [21].

According to [21], attenuation due to conductor loss for the TM1 mode is significantly higher than that for the TE1 mode in parallel plate waveguide.

To quantify this effect for the 10GHz lens 1 with a plate spacing of a = 19.05mm, and a frequency of 10GHz, the wave number k = 201m^{-1}. Thus, ka/π = 1.27. Referring to the curves for attenuation loss for the TE1 and TM1 modes in [21], it is seen that

$$\alpha_c = 1.25\frac{R_s}{\eta d} \tag{13}$$

This article has been accepted for publication in a future issue of this journal, but has not been fully edited. Content may change prior to final publication. Citation information: DOI 10.1109/TAP.2015.2435037, IEEE Transactions on Antennas and Propagation

for the TE1 mode and

$$\alpha_c = 3\frac{R_s}{\eta d} \tag{14}$$

for the TM1, mode, where d is the plate spacing (denoted by "a" elsewhere in this document), η is the impedance of free space, and R_S is the resistance of the material..

The attenuation due to conductor loss for the TE1 mode and TM1 mode for conductivities at 10GHz of aluminum and for the UNM CFRP/CNT with a conductivity of 726 S/m is shown in Fig. 25

material	**σ(S/m)**	**δ (m)**	**R_s(Ω)**	**α_c (Np/m) (TE1)**	**α_c (Np/m) (TM1)**
Aluminum	$2.5x10^{7}$	$1.0x10^{-6}$	0.0397	0.007	0.017
UNM CFRP	$7.6x10^{2}$	$1.8x10^{-4}$	7.20	1.26	3.02

Table 1 Attenuation Due to Conductor Loss for Al and CFRP composite

The attenuation due to conductor loss for aluminum for either the TE1 or TM1 mode is insignificant; however it becomes significant for the conductivity of the CFRP composite. For the TE1 mode, it is clear that the attenuation due to conductivity for the CFRP/CNT composite material is not sufficient to affect the focusing properties of the lens (see Figs. 20 and 21). However, the higher attenuation for the TM1 mode would help to mitigate propagation of this mode in the waveguide.

The width of the large L-Band lens near the outer edge of the lens is close to 1.2 m. The attenuation due to conductivity for the TM1 mode across this path length for aluminum would be αc = .02 Np, or about -16dB which is negligible. For the carbon fiber compound, it would be αc = 3.63 Np or about 6dB; which reduces the power available for radiation from the TM1 propagating mode by a factor of 4.

The conclusion is that carbon fiber reinforced polymer composites may be the material of choice over a metal for larger, lower frequency lenses because of their lower density and higher resistivity to the TM1 mode compared to aluminum; however, this would need to be further explored through experiment.

V. SUMMARY/CONCLUSIONS

A high power microwave zoom antenna comprising a moderate gain feed horn antenna and two parallel plate waveguide antennas has been successfully designed and demonstrated through experiment and simulation. This is a novel concept; there is nothing else in existence that can provide this capability for high power microwave applications. The antenna radiates a collimated beam of linearly polarized electromagnetic waves with continuously variable diameter with an achievable zoom ratio of 10:1.

This zoom antenna works with any HPM source with as much as 10% bandwidth that can produce a TE10 mode into a waveguide output.

The parallel plate waveguide lenses have relatively high tolerance to warping and twisting and are sufficiently lightweight to employ in a field-able system. Simple spherical lenses were demonstrated to work well in this application, resulting in low complexity and therefore low cost in design. For minimal cost, aluminum is a preferable material for the lens, with dielectric rods and spacers to provide the support structure. Sixteenth inch aluminum plates are sufficiently rigid with this construction to employ in even very large lenses.

If overall weight is a more important consideration than cost, the plates can be constructed of special carbon fiber reinforced polymer composites, which could reduce the weight by at least 25% and conceivably by as much as a factor of 5, depending on the material. It was observed through simulation that this material would not be too lossy to serve as plates for lens construction. In fact, the lower conductivity of the carbon fiber compounds would aid in mitigating undesirable TM modes in the lens that may be induced for very close spacing between the feed horn aperture and the first lens due to longitudinal fields present in the near field of the horn antenna.

For future work, it is hoped to fabricate and test lenses made with the CFRP composite.

VI. REFERENCES

[1] J. Lawrance and C. Christodoulou, "A High Power Microwave Zoom Antenna with Metal Plate Lenses", in *2014 IEEE Antennas and Propagation Society International Symposium*, Memphis, TN, 2014, p. 1652

[2] H. Lu, "Variable Beamwidth and Zoom Contour Beam Antenna Systems", U.S. Patent 6,414,646, July 2, 2002.

[3] R. F. Schmidt, "Variable Beamwidth Antenna", U.S. Patent 3938162, February 10, 1976

[4] L. K. DeSize et al, "Reflector Antenna Zoom Techniques", Airborn Instruments Lab, Deer Park, NY, Feb 1967

[5] W. E. Kock, "Metal-Lens Antennas," Proceedings of the I.R.E. (34) 1, pp. 828–836, Nov 1946

[6] J. D. Kraus, *Antennas*, 2nd Ed., McGraw Hill, NY, 1988, pp. 661-683

[7] S. Silver, "Microwave Antenna Theory and Design" MIT Radiation Laboratory Series, Vol 12, Ch. 11, pp. 389-412

[8] C.J. Sletten, *Reflector and Lens Antennas; Analysis and Design Using Personal Computers*, 1st ed., Artech House, MA, 1988, pp. 262-289

[9] L. V. Blake and M. W. Long, *Antennas: Fundamentals, Design, Measurement*, 3rd Edition, SciTech Publishing, Inc., NC, 2009, pp. 264-266

[10] J. D. Kraus, *Antennas for All Applications*, 3rd Ed., McGraw Hill, NY, 2002, pp. 626

[11] P. Wade and M. Reilly, "Metal Lens Antennas for 10 GHz," *Proceedings of the 18th Eastern VHF/UHF Conference*, ARRL, May 1992, pp. 71-78.

[12] Airy Disk, n. d., Retrieved 24 April, 2015 from http://en.wikipedia.org/wiki/Airy_disk

[13] A. Bojovschi et al, "Analysis of a Carbon Fibre Reinforced Polymer Slotted Waveguide Array Fed By a Loop Type End Launcher", *Microwave Conference Proceedings (APMC)*, 2013 Asia-Pacific, pp. 476-478

[14] T. Seidel et al, "The Anisotropic Conductivity Unidirectional Carbon Fibre Reinforced Polymer Laminates and Its Effect on Microstrip Antennas", *Proceedings of Asia-Pacific Microwave Conference*, 2010.

[15] M. J. Akhtar et al, "A Multi-Layered Waveguide Technique for Determining Permittivity and Conductivity of Composite Materials"., *Proceedings German Microwave Conference*, 2005, pp. 37-40

[16] C. L. Holloway et al, "Analyzing Carbon-Fiber Composite Materials with Equivalent Layer Models", *IEEE Transactions on Electromagnetic Compatibility*, Nov 2005, Vol. 47, No. 4, pp. 833-844,

[17] Y. J. Kim et al, "Electrical Conductivity of Chemically Modified Multiwalled Carbon Nanotube/Epoxy Composites", *Carbon*, 2005; 43(1), pp. 23-30

[18] A. Bojovshi et al, "The Reflectivity of Carbon Fiber Reinforced Polymer Short Circuit Illuminated by Guided Microwaves", *Applied Physics Letters*, 103, 111910 (2013)

[19] H. Dai et al, "Probing Electrical Transport in Nanomaterials: Conductivity of Individual Carbon Nanotubes", *Science*, 272-5261, pp. 523-526

[20] W. D. Burnside and C. W. Chuang, "An Aperture-Matched Horn Design," *IEEE Transactions on Antennas and Propagation*, AP-30, pp. 790-796, July 1982

[21] D. M. Pozar, *Microwave Engineering*, 3rd Ed, John Wiley and Sons, Inc., New Jersey, 2005, p. 105